NEW METHOD OF TEMPERATURE-RAMPING, ISOBARIC EXPERIMENTS TO STUDY THE HYDRATE FORMATION AND DECOMPOSITION

Guillaume Besnard, Kyoo Y. Song, Joe W. Hightower, Riki Kobayashi, Doug Elliot*, and Roger Chen*, Department of Chemical Engineering, MS-362, Rice University, 6100 Main Street, Houston, Texas 77005-1892.
* International Process Services, Inc., a subsidiary company of the Bechtel Corp., P. O. Box 2166, Houston, Texas 77252-2166.

Key Words: Hydrate, Methane, Solubility, Enthalpy, Entropy

Gas hydrate formation and decomposition involving methane in water has been studied in a series of temperature-ramping, isobaric, variable-volume experiments. Results obtained have provided novel information on (1) gas solubility in the liquid phase at temperatures in the vicinity of hydrate formation, (2) derived thermo-physical properties such as enthalpy, entropy, etc., and (3) details of the mechanism of hydrate formation/decomposition. Also, heats of dissolution/formation may be obtained indirectly from these results. An attempt was made to overcome experimental difficulties which had been imposed by the appearance of the hydrate solid phase. Such detailed solubility information will add substantially to the scarce data currently available in the literature.

INTRODUCTION

Though the existence of hydrates was demonstrated by Davy (1) in the early part of the nineteenth century, current interest dates from 1934 when Hammerschmidt (2) discovered that hydrates were responsible for plugging natural gas lines. This discovery stimulated numerous studies to determine the hydrate structure and its formation and decomposition conditions. The authors have recently employed a temperature-ramped, isobaric (constant pressure), variable-volume technique that is capable of providing continuous details of hydrate formation and decomposition. Furthermore, the method enables a straightforward calculation of solubility of the hydrate former in the host phase which may be pure water or aqueous solutions.

Information on the solubility of gases like CH_4 in pure water is very useful for the calculation of some derived thermo-physical properties such as the enthalpy of solution, the enthalpy of formation, and the entropy change of the solution. Gas solubility has been extensively studied (5-12) and found to be extremely low. It has been generally reported for temperatures above ambient. However, the same information at the low temperatures and high pressures is very scarce. The solubility of hydrate formers, such as methane, ethane, carbon dioxide, etc., is not easily measurable due to the appearance of the hydrate solid phase, metastable phases, etc. The increase of the solubility with decreasing temperature can be explained by the formation of an ice-like structure (i.e. pentagonal dodecahedra) in the solvent (13-16). Another explanation is that displacement of solvation equilibrium occurs with changes in temperature ($\Delta H_{solv}<0$) and that the solute introduces low entropy structures in water (15-17). The solvation of gas, R, is considered as a relaxation to the equilibrium process described as follows:

$$R + nH_2O = R(H_2O)n.$$

First introduced by Pauling (3) in 1957 and expanded in recent studies (12-18), a concept has developed that the hydrate structure has a geometry similar to basic water structure and the liquid forms its own "buckyballs". The "buckyball" includes 21 water molecules, 20 of which form a pentagonal dodecahedron with one molecule in the middle to add stability to the cage. At ambient temperature, it was proved that these structures are metastable and flicker in and out of existence (19). Sloan and Fleyfel (4) in 1991 proposed a kinetic model of gas hydrate formation from ice assuming that during the nucleation period considerable metastability occurs because of the forming and breaking of structures. Although many more detailed studies are required, our experiments have made it possible to detect the different steps suggested by Sloan et al. (4).

The solubilities of methane and ethane in water at low pressures (3.45 and 0.66 MPa, respectively) have been reported earlier (20). This paper reports results for methane obtained at higher pressures (10.48 and 13.93 MPa) in the temperature range 291.2 to 278.2 K, which includes the hydrate formation conditions, and divergence of these measurements from solubility predicted by Henry's law is presented.

EXPERIMENTAL SECTION

Experimental Apparatus

Calorimeter

A differential calorimeter, which is a variation of the common heat flux calorimeter (21), used in these studies consists of two symmetrical containment vessels, both thermally insulated from the surrounding aluminum block. One containment vessel serves as the sample cell while the other vessel serves as a reference. The surrounding block temperature is ramped at a fixed rate, (by using heating and/or refrigeration), allowing a steady-state heat flux between the sample vessel and the surroundings. But the calorimeter can also be used in an "isoperibolic" operation where the surrounding block is held at a constant temperature (22). The calorimeter is equipped with an internal electrical conductivity cell to track the amount of water in the hydrate and liquid phase by monitoring the conductivity of a dilute KCl solution during hydrate formation.

Moreover, any heat exchange between the containment vessel and the surrounding block occurs almost exclusively by conduction and is measured by two thermopiles. The resulting differences in voltage for the two thermopiles represent the differential heat flux for the two containment vessels. Integrating this voltage over time gives the total heat transfer associated with "the event." However, for this work, the heats of dissociation have been calculated from the solubility of methane since the thermopile values were not reliable enough to provide us with consistent data. Figure 1 shows the apparatus and the pressure-maintaining system.

Computer/data acquisition

Performance of the calorimeter strongly depends on the control and data acquisition program for the computer. Our program is capable of handling various data acquisitions while controlling the pressure and the temperature precisely. The program has been written in "Visual Basic" and can set heater load and pump position (i.e. volume of gas added to the cell during the ramping experiments). The pressure is controlled every four seconds, and the data are collected every minute, allowing precise control of the temperature-ramping, isobaric experiments. Measurements were made during the data acquisition from two pressure transducers, three PRTs, a thermopile, and an electrical conductivity device.

The stepping motor, Genrad RLC Digibridge, HP multimeter, and Keithley digital multimeter are controlled via an IEEE interface. Pressure transducers and a temperature controller are interfaced via an RS232. Figure 2 shows a block diagram of the control and data acquisition systems.

Experimental Procedure

The right cell of the calorimeter shown in Figure 1 is first charged with roughly 650 grams of the dilute aqueous potassium chloride solution (~0.004 normal) prepared with ultra-pure water (17.0 megaohm-cm resistance) and Baker Analyzed Reagent grade salt. This solution fills approximately two thirds of the cell, in order to insure that the electrical conductivity cell be immersed, and magnedrive propellers provide vigorous mixing of the cell contents. After the system has been evacuated to remove air, methane gas is introduced to the system comprising the calorimeter cell, the right pump, and the pressure lines.

The fundamental measurement is the change in volume of the digital pump during the temperature-ramping experiments while the pump is controlled by a stepping motor to maintain the pressure constant. The stepping motor is actuated by a digital-based driver which is controlled by a computer through the IEEE interface. The system consists of the stepping motor, Digidrive, transformer, and 2100 Indexer with an IEEE interface. Flow rates range from 5 to 96 cc/min has been achieved. The pump is able to add to or withdraw gas from the cell at very precise rates. But precise control of the isobaric operation strongly depends on the pressure transducer that closes the loop. They are rated at 10,000 psia with an accuracy of 0.07%. The displacement of the plunger of the pump gives us the volume of methane gas added to the cell, hence the solubility of methane in water-rich phase.

RESULTS AND DISCUSSION

Plots of changes in the system volume versus temperature, as shown in Figure 3, present typical experimental results in a way similar to that used previously (20). However, the current pressures (10.48 and 13.93 MPa) are much higher than the previous one, 3.45 MPa. Figure 3 shows different regions along the curve which are:

a) Cooling

(1) An interstitial solubility where gas is dissolved into water according to

Henry's law.
(2) Solubility of the gas begins to increase beyond that accounted for by Henry's law.
(3) The gas intake by the water increases, and this point is commonly called a catastrophic temperature(Tc). The solubility continues to increase.
(4) Catastrophic hydrate formation occurs, and the amount of solid present in the water has drastically increases.
(5) Solidification starts but the magnetic stirrer is still running.

b) Heating

(6) Dissociation of the hydrates begins. The hydrate crystals start melting and the volume maintains a constant value.
(7) The volume drops very fast and the hydrates are almost completely decomposed. The volume returns to its initial value.

Figures 4 and 5 show calculated methane solubility of (log[mole fraction CH_4 in water]) at 13.93 MPa (2020 psia) plotted vs. (1/T) and Ln (T), respectively, while Figure 6 presents the solubility of methane ($1000 * X_{CH4}$) vs. temperature at 10.48 MPa (1520 psia). Table 1 provides the solubility of methane gas in pure water obtained during the temperature-ramping experiment at a rate of 1.2°C/hr, for both pressures of 10.48 and 13.93 MPa. Table 2 presents the changes of enthalpy and entropy obtained by plotting Ln(x) versus 1/T (T in K) from the relation of

$$d\,Ln(x) / d\,(1/T) = -\Delta H/R$$

and Ln (X) vs. Ln (T) (again, T in K) by the relation:

$$d\,Ln(x) / d\,ln(T) = +\Delta S/R\ .$$

We had to extrapolate the available literature data of methane solubility in water far above hydrate formation condition (5) to establish a reference for the solubility of methane in pure water in the low temperature region.

Figures 3 and 4 demonstrate a sudden increase of the gas solubility from the extrapolated values. Below 17°C, the liquid solution becomes supersaturated with methane gas. Song et al. (20) attributed this increase to a "sorption" effect with the ordering of water molecules into an ice-like structure with the water molecules surrounding the hydrocarbon molecules. These ordered structures result from contact of the hydrocarbon with water which induces small dipole moments into the hydrocarbon molecules and allows some ordering through weak dipole-induced dipole interactions with the water. The number of water molecules affected by the interaction with the hydrocarbon solute is related to the size of the guest molecule, i.e. the contact surface of the guest molecule. Therefore, the size of the "ice-like" structures will increase with the size of the hydrocarbon (24).

At Tc, the catastrophic temerature at which hydrate crystals start to form, the solubility is increased by 78 % for 10.48 MPa and 51 % for 13.93 MPa. After hydrate crystals are formed, the solubility still increases, showing a high level of supersaturation of methane gas in liquid water, which started just before and just after Tc. These solubility measurements emphasize the crystallization-like process taking place during hydrate formation. The dissolved gas molecules form the nuclei which initiate the process of hydrate precipitation and crystal growth. One might state that around Tc, the nucleation occurs as a result of a fluctuation in free energy due to the local temperature and pressure fluctuations, of sufficient importance to surmount the free energy barrier (12).

From an energy point of view, the changes of enthalpies and entropies are negative and in agreement with reported values (20, 22, 25). The changes in enthalpy and entropy, as the temperature approaches Tc, could be compared with ice formation on one hand and experimental heats of dissociation on the other. The enthalpy of dissociation for the methane hydrate at 13.93 MPa is very close to the enthalpy of dissolution of the same gas when Tc is approached, as found previously (12). Moreover, the comparison of the entropies of solution derived here with corresponding values based on the same standard state for gases in non-polar solvents at 25°C shows that the entropies of solution in water are all negative by a large amount. The partial molal entropy of solution is influenced by the size of the cavity created by the gas molecules when the estimate of the cavity size is made by bond distances. Frank and Evans (15), and Song el al. (20) have demonstrated that the large negative values for partial molal entropies of solution of non-polar gases in water can be understood as the creation of a more highly ordered state in water or "icebergs". As the temperature is increased, these quasi-ice-like structures break up and ΔS becomes positive.

CONCLUSION

A fully automated calorimeter with some modifications has facilitated isobaric (constant pressure), variable-volume, and temperature-ramped experiments, and the experimental procedure has enabled us to elucidate discrete steps involved in the hydrate formation and decompostion for a high pressure methane-water system in a continuous manner.

Simultaneously, the measured volumes were utilized to determine directly methane gas solubility in the water phase in a way that minimizes uncertainties associated with the appearance of the solid hydrate phase.

Of importance, it has been confirmed that the solubility of methane gas in water in the vicinity of the incipient hydrate formation temperature is much greater than that would be predicted by Henry's law, a frequently-used conventional calculation procedure.

Finally, the obtained solubility was used to calculate derived thermo-physical properties, i.e. changes of enthalpy and entropy of the solution.

LITERATURE CITED

(1) Davy, H. *Phil. Trans. Roy. Soc.*, London **1811**, *101*, 1.
(2) Hammerschmidt, E. G. *Ind. Eng. Chem.* **1934**, *26*, 851.
(3) Pauling, L. The Structure of Water Hydrogen Bonding. Hadzi, D. Pergamon Press, **1959**.
(4) Sloan, E. D.; Fleyfel, F., *J. AIChE* **1991**, *37*, 1281.
(5) Culberson, L.; McKetta, J. *AIME Trans* **1950**, *189*, 1.
(6) Kobayashi, R. *Vapor-Liquid Equilibrium in Binary Hydrocarbon-Water systems.* Ph-D Dissertation, University of Michigan, **1951**.
(7) Katz, D.L.; Cornell, D.; Vary, J.; Kobayashi, R.; Elenbaas, J.R.; Poettman,F.H.; Weinang, C.F. *Handbook of Natural Gas Engineering* **1959.**
(8) Clever, H.L.; Han, C.H. *ACS Symp. Ser.* **1980**, *133*, 513.
(9) Clever, H.L.; Battino, R. *Role. Data Sci. Prog.* **1986**, *9*, 209.
(10) Battino, R. *Sol. Data Ser.* **1986**, *24*, 1.
(11) Battino, R. *Sol. Data Ser.* **1987**, *27*, 1.
(12) Feneyrou, G. *Elucidation of the Formation and Decomposition of Clathrate Hydrates of Natural Gases through Gas solubility Measurements.* M.S Dissertation, Rice University, **1996** .
(13) Klotz, I.M. *In Protein Structure and Function,* Brookhaven Symposia in biology **1960**, *13*, 25.
(14) Patterson, D.; Barke, M. *J. Phys. chem.* **1976**, *80*, 2435.
(15) Frank, H.S.; Evans, M.W. *J. Chem. Phys.* **1945**, *13*, 507.
(16) Kauzmann, W. *Adv. Protein Chem.* **1959**, *14*, 1.
(17) Nemety, G.; Scheraga, H.A. *J. Phys. Chem.* **1962**, *36*, 3401.
(18) Fleyfel, F.; Song, K.Y.; Kook, A.; Martin, R.; Kobayashi, R. *J. Phys. Chem.* **1993**, *25*, 6722.
(19) Bernal, J.D. *Royal Society on Physics of Water and Ice* published in Hydrogen Bonding, Pergamon Press **1957.**
(20) Song, K.Y.; Feneyrou, G.; Fleyfel, F.; Martin, R. Lievois, J.S.; Kobayashi, R. *Solubility Measurements of Methane and Ethane At and Near Hydrate Conditions, in press,* Fluid Phase Equilibria **1996.**
(21) Calvet, E.; Prat, H. *Recents Progres en Microcalorimetrie* Dunod Edition Paris **1958.**
(22) Lievois, J.S. *Development of an Automated, High Pressure Heat flux Calorimeter and its Application to Measure the Heat of Dissociation of Methane Hydrate.* Ph-D Dissertation, Rice University, **1987.**
(23) Frank, H.S.; Wen, W.Y. *Discussion Faraday Society* **1957**, *24*, 133.
(24) Himmelblau, D.M. *Partial Molal Heats and Entropies of Solution for Gases Dissolved in Water from the Freezing Point to Near the Critical Point.* J. Phys. Chem. **1959**, *63*, 1803.
(25) Rettich, T.R.; Handa, Y.P.; Battino, R.; Wilhem, E. *Solubility of Gases in Liquids. High-Precision Determination of Henry's Constants for Methane and Ethane in Liquid Water at 275 to 328 K* J. Phys. Chem. **1981**, *85*, 3230.
(26) CSMHYD - hydrate program developed by the Colorado School of Mines (Dendy E. Sloan), available through the Gas Processors Association (GPA), Tulsa, Ok.

Table I. Solubility of Methane Gas in Water (Obtained from Temperature-Ramping (1.2 °C/hr), Variable-Volume, Isobaric Experiments)

pressure, MPa a (psia)	temp., K (°C)	sol. of CH_4, X_{CH4} *1000	pressure, MPa a (psia)	temp., K (°C)	sol. of CH_4, X_{CH4} *1000
10.48	291 (18.0)	2.04	13.93	292 (19.0)	2.96
(1520)	289 (16.0)	2.41	(2020)	290 (17.0)	3.22
	288 (15.0)	2.61		289 (16.0)	3.92
T^a =11.6 °C	285 (12.0)	3.62	T^a =14.6 °C	289 (15.5)	4.23
T^b=16.0 °C	285 (11.6)	4.09	T^b =18.0°C	288 (14.6)	5.03
T* =13.8 °C	284 (11.0)	4.45	T* =16.24°C	287 (14.0)	6.68
	283 (10.0)	5.17		286 (13.0)	11.29
	282 (9.0)	5.92		285 (12.0)	6.72
	280 (7.0)	7.54		283 (10.0)	25.70
	279 (6.0)	9.17		280 (7.0)	37.20
	278 (5.0)	11.41		279 (6.0)	44.95
				278 (5.2)	52.44
	298 (25.0)[c]	1.98			
				298 (25.0)[c]	2.62

a initial hydrate formation temperature,
b final decomposition temperature,
* predicted from hydrate program of Colorado School of Mines (22),
c obtained from Culberson and McKetta (1).

Table II. Derived Thermo-Physical Properties of a Methane-Water System (Obtained from Solubility Measurements)

pressure, MPa a (psia)	range of temp., °C	change of enthalpy, ΔH, KCal/mole of gas	change of entropy, ΔS, Cal/mole.K
10.483	16.0 to 12.0	-16.8	-58.6
(1520)	12.0 to 11.6	-47.7	-170.5
T^a = 11.6 °C	11.6 to 7.0	-21.1	-74.7
T^b =16.0 °C	7.0 to 5.0	-32.0	-115.9
T* =13.8 °C			
13.931	19.0 to 17.0	-7.1	-24.4
(2020)	16.0 to 14.6	-27.5	-95.2
T^a = 14.6 °C	14.6 to 13.0	-87.8	-308.9
T^b = 18.0 °C	12.0 to 6.0	-26.1	-92.3
T* = 16.24 °C			

a initial hydrate formation temperature,
b final decomposition temperature,
* predicted from hydrate program of Colorado School of Mines (22).

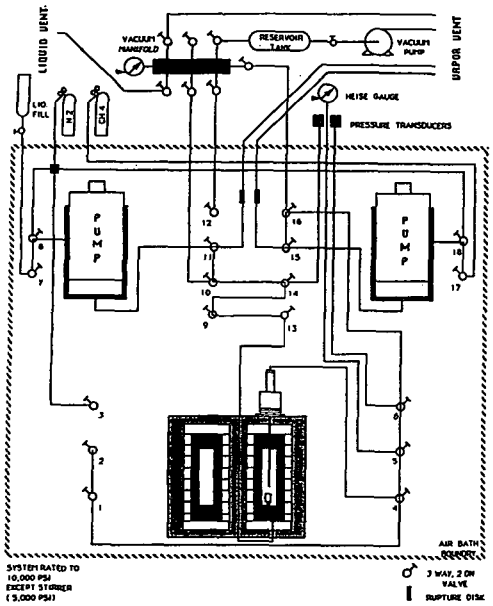

Figure 1. Calorimeter apparatus used for temp.-ramped, isobaric, and volume-variable experiments.

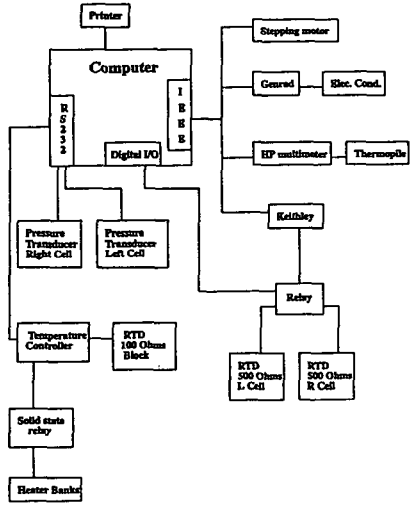

Figure 2. Block diagram of pressure and temperature controls and data logging system.

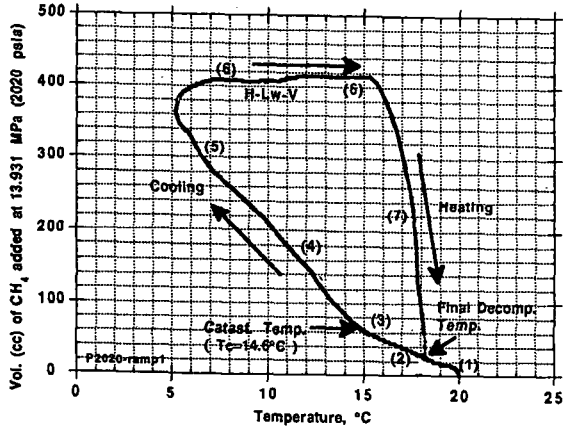

Figure 3. Change of system vol. vs. temp. for a methane and water system at 13.931 MPa (2020 psia) when the air bath temp. was ramped at 1.2°C/hr.

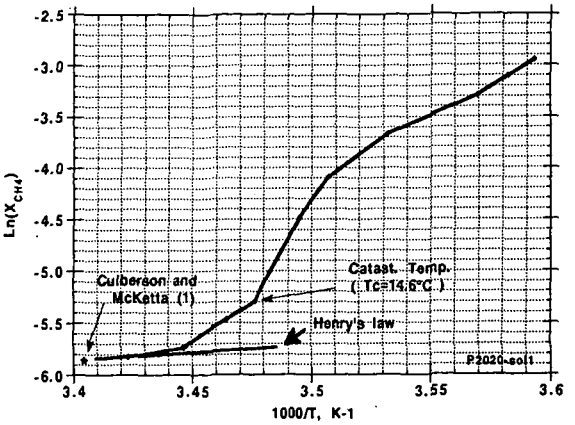

Figure 4. Logarithm of solubility (mole fraction) of methane in the water phase vs. reciprocal of the absolute temp. for a methane and water system at 13.931 MPa (2020 psia).

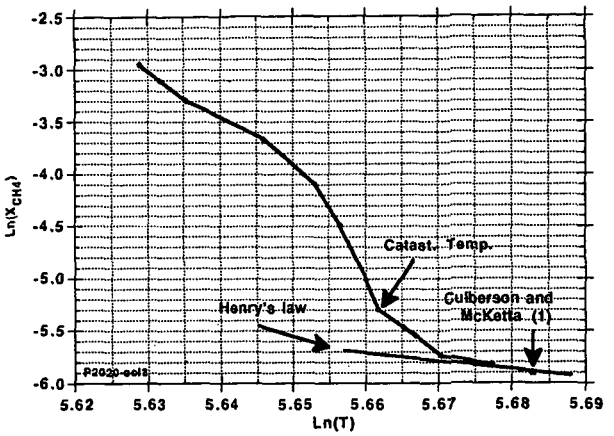

Figure 5. Logarithm of solubility (mole fraction) of methane in the water phase vs. logarithm of absolute temp. for a methane and water system at 13.931 MPa (2020 psia).

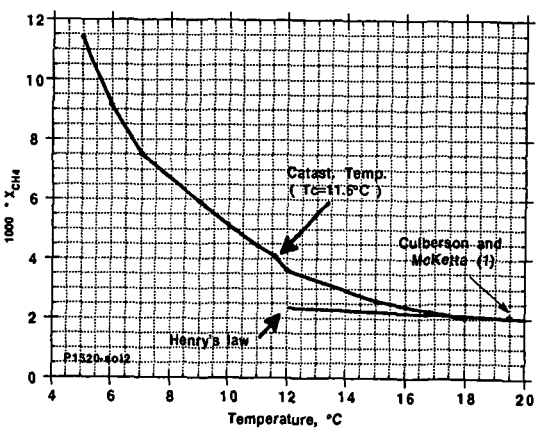

Figure 6. Solubility (mole fraction) of methane in the water phase vs. temp. for a methane and water system at 10.483 Mpa (1520 psia).